

JOM 23859

# Preparation and crystal structures of the complexes $(\eta^5\text{-C}_5\text{H}_4\text{CPh}_2\text{-}\eta^5\text{-C}_{13}\text{H}_8)\text{MCl}_2$ ( $\text{M} = \text{Zr, Hf}$ ) and the catalytic formation of high molecular weight high tacticity syndiotactic polypropylene \*

Abbas Razavi

*Fina Research, Centre de Recherche du Groupe Petrofina, Zone Industrielle C, B-7181 Feluy (Belgium)*

Jerry L. Atwood

*Department of Chemistry, The University of Alabama, Tuscaloosa, AL 35487-0336 (USA)*

(Received May 21, 1993)

## Abstract

The reaction of  $\text{MCl}_4$  ( $\text{M} = \text{Zr, Hf}$ ) with the dilithium salt of 1-cyclopentadienyl-1-fluorenyl-1,1-diphenylmethane in pentane at ambient temperature leads to the formation of the complexes  $(\eta^5\text{-C}_5\text{H}_4\text{CPh}_2\text{-}\eta^5\text{-C}_{13}\text{H}_8)\text{MCl}_2$ . NMR and X-ray diffraction data confirm that the fluorenyl groups are  $\eta^5$ -bonded in these complexes. When activated with aluminoxane or other appropriate ionizing agents both complexes catalyze the stereospecific polymerization of propylene to syndiotactic polypropylene of high molecular weight and tacticity.

## 1. Introduction

Since the discovery of the first stereorigid chiral ansa metallocene complexes [1,2] and their application as homogeneous catalysts in stereospecific polymerization of  $\alpha$ -olefins to polymers with stereoregular microstructures, numerous papers have been published discussing the various parameters that could control the activity of the catalyst and the stereospecificity of the polymerization reaction [3]. The bridge in the ansa metallocene has been considered as an instrument to maintain the symmetry of the corresponding active cationic species that are formed during the initial stages of the polymerization [4]. Its influence on the catalytic olefin polymerization was supposed to be of minor extent because of its remoteness from the coordination sphere of the transition metal. In this paper we demonstrate the enormous influence of the substituent in the  $\text{C}_1$  bridge on the activity and stereoselectivity of the

homogeneous polymerization reaction of propylene and the molecular weight and the stereoregularity of the resulting polypropylene.

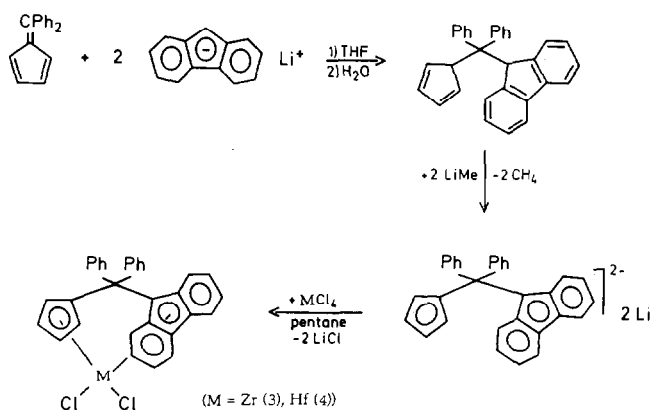
## 2. Results and discussion

The isopropylidene complexes  $(\text{C}_5\text{H}_4\text{CMe}_2\text{-C}_{13}\text{H}_8)\text{MCl}_2$  ( $\text{M} = \text{Zr}$  (1),  $\text{Hf}$  (2)) are well studied catalyst precursors for the polymerization of propylene to syndiotactic polypropylene [5–7]. The corresponding phenyl substituted complexes 3 and 4 can be prepared according to Scheme 1. Complexes 3 and 4 have been characterized by their  $^1\text{H}$  NMR spectra and X-ray structures.

The  $^1\text{H}$  NMR spectra in  $\text{CD}_2\text{Cl}_2$  of 3 and 4 are almost identical; deviations are in the range of 0.01–0.04 ppm. Figure 1 shows the  $^1\text{H}$  NMR spectrum of 3 (bottom) contrasted with the  $^1\text{H}$  NMR spectrum of 1 (top). The various signals have been assigned on the basis of a correlated  $^1\text{H}/^{13}\text{C}$  2D NMR spectrum and in combination with an NOE difference spectrum. The two virtual triplets at  $\delta = 5.80$  and 6.37 ppm ( $J(\text{H, H}) = 2.7$  Hz) results from an AA'BB' pattern and are due to protons in positions 1 and 2 in the  $\text{C}_5\text{H}_4$  group. The fluorenyl protons 3, 4, 5, and 6 give rise to a doublet

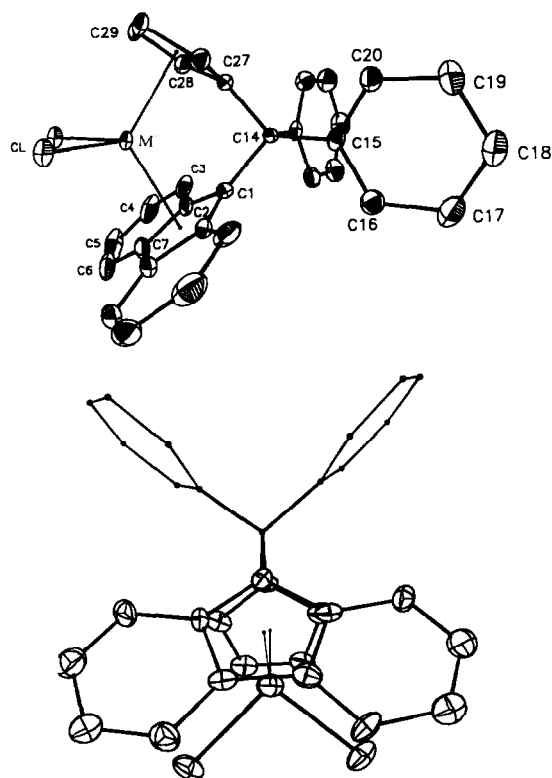
Correspondence to: Dr. A. Razavi.

\* Dedicated to Professor E.O. Fischer on the occasion of his 75th birthday.



Scheme 1.

triplet-triplet doublet pattern appearing at  $\delta = 6.43$ , 6.99, 7.56 and 8.19 ppm respectively. The coupling constants for the doublets and triplets are *ca.* 8.5 Hz. All protons of the phenyl substituents are diastereotopic and give rise to five distinct signals at  $\delta = 7.32$ , 7.35, 7.47, 7.88 and 7.95 ppm. A comparison with the <sup>1</sup>H NMR spectrum of **1** reveals that in both complexes the protons of the C<sub>5</sub>H<sub>4</sub> show the same coupling pattern and similar chemical shifts. The corresponding protons belonging to the C<sub>13</sub>H<sub>8</sub> groups for **3** and **1**, however, have been subjected to different shielding and deshielding forces (as a result of the magnetic field anisotropy caused by the ring currents of the two phenyl substituents in the bridge) and appear at differ-

Fig. 2. Two perspective views of the molecular structures of **3** and **4** in the crystalline state.

ent part of the magnetic field (*cf.* Fig. 1). Proton 3 (closest to the phenyl groups) in complex **3** has experienced the most dramatic upfield shift. Its signal appears at 6.43 ppm and is more than 1.5 ppm shifted to higher field. The signal related to proton 4 too is shifted to higher field by about 0.5 ppm in complex **3**. The chemical shift variations for protons 5 and 6 are, however, less pronounced.

### 2.1. X-ray structures of **3** and **4**

The molecular structures of **3** and **4** are portrayed in Fig. 2. Important bond distances and bond angles are given in Table 1. Complexes **3** and **4** have almost identical structures therefore only the structure of **3** will be discussed. As in the case of similar, previously reported metallocenes, having a C<sub>5</sub>H<sub>4</sub>CR<sub>2</sub>C<sub>13</sub>H<sub>8</sub> chelating ligand system [6–8], the least-squares planes defined by the two C5 fragments in **3** are inclined towards the zirconium atom with respect to C(14)–C(1) and C(14)–C(27) vectors. The effect is more pronounced for the cyclopentadienyl ring than the fluorenyl group. The unexpectedly small angle at the diphenylmethylidene carbon C(1)–C(14)–C(27) = 99.1° is probably due to the metalloceneophane character. The angle formed between the two centroids and the zirconium, Flu–Zr–Cp (Flu = fluorenyl, Cp =

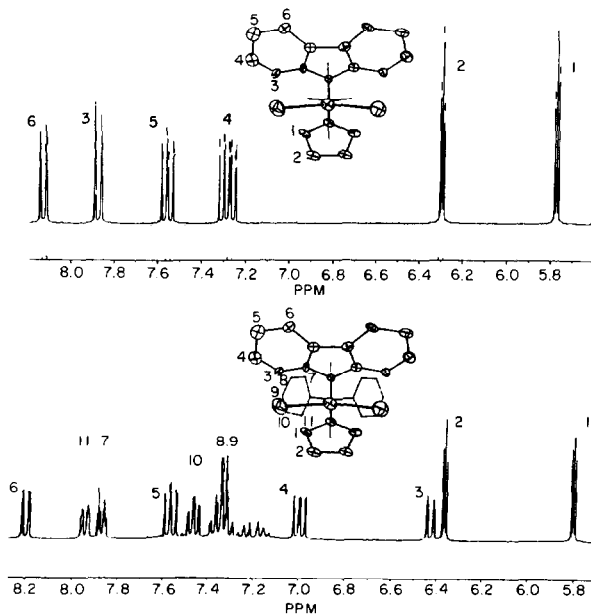
Fig. 1. Comparison of the <sup>1</sup>H NMR spectra of **1** and **2** (in CD<sub>2</sub>Cl<sub>2</sub>, 25°C) and assignment of the signals in the range of 5.8–8.3 ppm.

TABLE 1. Selected bond lengths (Å) and bond angles (°) for **3** and **4**, with e.s.d.s<sup>a</sup>

	<b>3</b>	<b>4</b>
M-Cl	2.424(2)	2.403(2)
M-C(1)	2.417(8)	2.410(1)
M-C(2)	2.513(6)	2.511(9)
M-C(7)	2.680(6)	2.670(1)
M-C(27)	2.452(8)	2.440(1)
M-C(28)	2.450(6)	2.439(9)
M-C(29)	2.523(6)	2.505(9)
Z(Flu)-M-Z(Cp)	117.6°	118.2°
Cl-M-Cl	95.9°	95.6°
C(1)-C(14)-C(27)	99.1°	99.6°

<sup>a</sup> Z(Flu) and Z(Cp) denote the centres of the five membered rings of the fluorenyl and the cyclopentadienyl groups.

cyclopentadienyl), 117.6°. The smaller values for these two angles compared to the corresponding values for **1** are consistent with a displacement of the Zr atom further out of the mouth of the ligand. The Cl-Zr-Cl angle of 95.9° is palpably smaller than the corresponding angles in **1** but lies within the range of predicted and observed values for d<sup>0</sup> Group 4 metallocenes [9–12]. The Zr-Flu bonding has an  $\eta^5$  nature and the progressive increase in the Zr-C bond distance from bridge head carbon C(1) (2.417(8)) to C(2) (2.513(6)), and C(7) (2.680(6) Å) should be attributed to the non-bonding repulsive interaction between the two chlorine ligands and the dorsal carbon and hydrogen atoms of the two fluorenyl six membered rings, rather than to a hapticity change. A similar effect, though less pronounced, is observable for the Zr-C bond distances for distal carbon atoms in cyclopentadienyl ring. The Zr-C(29) and Zr-C(30) distance of 2.523(6) Å is about 0.02 Å larger than the Zr-C bond distance to the bridge head carbon. The non-bonding interactions between the  $\sigma$ -bonded terminal ligands and the ancillary atoms of the chelating ligands surrounding the active coordination sphere of the central metal (causing these bonds to lengthen) are pertinent for the stereoselectivity of the actual catalysts.

## 2.2. Polymerization behavior

Complexes **3** and **4** in combination with aluminoxane or other ionizing agents are excellent catalysts for promoting the polymerization of propylene to highly syndiotactic polypropylene. Table 2 compares the catalytic performance of **3** and **4** as well as their respective polymer analyses. The polymers produced with these two catalysts under similar polymerization conditions show a much higher molecular weight and a higher degree of stereoregularity than the polymers produced with syndiospecific systems **1** and **2**. The <sup>13</sup>C NMR

TABLE 2. Polymerization results and conditions<sup>a</sup> for **3** and **4**/MAO

Complex	mg	Pol. temp. (°C)	Activity (pol.g/g cat/h)	M <sub>w</sub> (×10 <sup>-3</sup> )	r (%)	Mp. (°C)
<b>1</b>	0.56	50	194000	133	96.0	138
<b>2</b>	4.78	50	54000	777	74.0	118
<b>3</b>	1.51	50	68200	560	97.5	139
<b>4</b>	6.30	50	11700	1950	90.3	101

<sup>a</sup> Propylene (1 l); 10 ml of 10 wt% MAO(Schering). The abbreviations have been explained in [6].

spectra and steric sequence distributions of syndiotactic polymers produced with **1** and **3** are contrasted in Fig. 3.

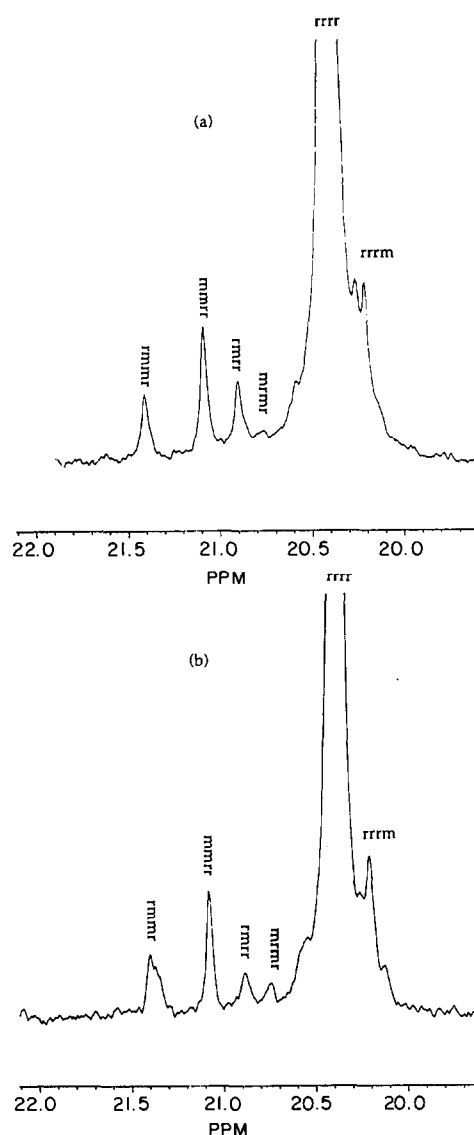


Fig. 3. The <sup>13</sup>C NMR spectrum of the methyl of syndiotactic polymers produced with **1** (a) and **3** (b) at 50°C in combination with MAO. TMS scale.

### 2.3. Mechanistic aspects of the polymerization and the influence of the diphenyl substituents on the polymer chain length and stereoregularity

A comparison of the polymer properties given in Table 2 for syndiotactic polypropylene produced with **3** and **4** as well as those reported previously for **1** and **2** reveals that, under similar polymerization conditions, **3** and **4** produce polymers with much higher molecular weights and somewhat higher tacticities though with lower activity. These tangible differences in the macro- and microstructure of the polymer are intimately related to the structural characteristics of the metallocene catalysts. This "catalyst structure -polymer property" relationship can be rationalized by the following interpretation of the analytical data obtained from catalyst precursors' static and dynamic parameters. Close inspection of the interatomic parameters and the results derived from various methods of NMR spectroscopy (Fig. 1) indicate, that the electromagnetic fields induced by ring currents of the phenyl groups in the C<sub>1</sub> bridge have caused a deformation of the electron clouds of the aromatic  $\pi$ -system of the fluorenyl six membered rings and a redistribution of the electron densities concentrated on different atoms (*cf.* <sup>1</sup>H NMR). These non-bonded, through-space interactions are probably also at the origin of the slight structural modifications of the molecule, the displacement of the transition metal further out of the mouth of the ligand (*vide supra*), and the greater exposure of its frontier orbitals.

The exposed orbitals are more diffuse and their orientation in space is affected by the new electronic requirement of the ligand. The alteration of the shape and the direction of the spatial extension of the frontier orbitals of the metal-alkyl cation (which is formed during the initial stages of the polymerization and persists throughout the propagation reaction as the active species) on the other hand will change the course of the polymerization reaction by requiring new reaction pathways. It has been proposed that this electronically and sterically unsaturated, highly reactive species is stabilized by agostic interactions with hydride anions positioned on the carbon atoms of the alkyl chain end  $\alpha$  or  $\beta$  to the transition metal acting as a ligand with a pair of electrons [11–16].

The occurrence and the frequency for each of these two interactions depends on the shape and the extension of the available frontier orbitals and can change the kinetics of the propagation, the mechanism of polymerization reaction, and affect dramatically the molecular weight and stereoregularity of the polymer chain. An  $\alpha$ -hydride agostic interaction that would maintain the active centre intact in the absence of the monomer yet would keep it receptive to coordination

of incoming monomer molecules for successive insertion is crucial for the formation of polymers with high molecular weights. However, a  $\beta$ -hydride agostic interaction would cause a rapid  $\beta$ -hydride elimination and would lead to the formation of chains with lower molecular weights or olefinic oligomers. The higher molecular weight of the polymer produced with **3** and **4** suggests strongly that the steric and electronic disturbances caused by the two phenyl substituents have rendered the frontier orbitals more accessible for an  $\alpha$  agostic rather than a  $\beta$  agostic interaction. Furthermore, the preferred  $\alpha$ -agostic interaction, according to a mechanism similar to that proposed by Brintzinger [16] (for isotactic system), would favour the formation of a more stereoregular polymer by placing the polymer chain in the right sector of the ligand framework for directing the incoming monomer to approach with the proper enantiofacial orientation. The lower activity of **3** and **4** compared to **1** and **2** could be also regarded as a consequence of the  $\alpha$ -hydride interaction which reinforces the M–C bond by decreasing its polarity thus lowering the pace of the insertion and propagation rates. Finally, similar melting points for polymers with different tacticities might at first sight appear strange but can be explained by the fact that any gain in crystallinity which would result from higher regularity is cancelled out by the increase of the length of the polymer and the more difficult process of aligning longer polymer chains.

### 3. Experimental details

All operations were performed under an inert gas atmosphere using glove box or Schlenk techniques. Pentane and methylene chloride were dried over calcium hydride, toluene and tetrahydrofuran (THF) over sodium/benzophenone. All solvents were freshly distilled before use. ZrCl<sub>4</sub> were obtained from Comprehensive Research Chemical Corporation, P.O. Box 4591, Anaheim, CA 92801, USA. 6,6-diphenylfulvene and fluorenyl (98% purity) were obtained from Aldrich and were used without further purification.

#### 3.1. Preparation of the ligand

Into a round bottom flask equipped with side arm, addition funnel and magnetic stirring bar 25 g (0.15 mol) of fluorene and 200 ml of THF were added. An equimolar amount of methylolithium in ethyl ether (1.4 M) was added in a 30 min period at room temperature. The resulting deep red solution was stirred for several hours until gas evolution had completely ceased. A solution of 34.54 g (0.15 mol) of 6,6-diphenyl fulvene in 100 ml THF was added dropwise. The resulting red THF solution was stirred overnight and treated subse-

quently with 200 ml with an ammonium chloride saturated water solution and stirred for 10 min. The organic layer was extracted several times with 100 ml portions of ethyl ether and the combined organic phases were dried over magnesium sulfate. After removal of the ether and recrystallization of the solid from a methanol/chloroform solvent mixture yielded 32.4 g (54.51%) of a white spectroscopic pure product.

### 3.2. Preparation of dianion

A 500 ml round bottom flask equipped with side arm, addition funnel, and magnetic stirring bar was charged with 25 g (0.042 mol) of **1** in 300 ml of THF. To this solution two equivalents of methyl lithium in diethyl ether (1.4 M) were added dropwise at room temperature. The resulting red solution was stirred at this temperature for 6 h, the THF then removed under vacuum and the residue washed with pentane to give the dilithiated compound as a yellow-orange powder in quantitative yield. The product was used without further purification.

### 3.3. Preparation of **3**

To a suspension of 0.025 mol (10 g) of **2** in 200 ml of dry pentane, in a 1 l round bottom flask equipped with a magnetic stirring bar was added a suspension of an equimolar amount of ZrCl<sub>4</sub> powder in 200 ml of pentane. The mixture was stirred at ambient temperature for 6 h. At the end of this period the colour of the slurry changed to red and the reaction was completed. The pentane was decanted and the remaining red solid

TABLE 4. Final fractional coordinates

Atom	x	y	z
Zr	0.18020(9)	0.7500	0.62782(4)
Cl	0.2139(2)	0.6314(1)	0.71257(8)
C(1)	0.2537(8)	0.7500	0.5043(4)
C(2)	0.3229(7)	0.6739(5)	0.5341(3)
C(3)	0.2981(8)	0.5811(5)	0.5267(4)
C(4)	0.386(1)	0.5255(7)	0.5642(4)
C(5)	0.490(1)	0.553(1)	0.6080(5)
C(6)	0.5148(9)	0.642(1)	0.6172(5)
C(7)	0.4313(7)	0.7027(6)	0.5810(3)
C(14)	0.1167(8)	0.7500	0.4636(4)
C(15)	0.0979(6)	0.8296(4)	0.4137(3)
C(16)	0.2078(6)	0.8585(4)	0.3721(3)
C(17)	0.1887(8)	0.9257(5)	0.3225(4)
C(18)	0.0620(9)	0.9645(5)	0.3144(4)
C(19)	-0.0471(8)	0.9369(5)	0.3552(4)
C(20)	-0.0298(7)	0.8693(4)	0.4047(3)
C(27)	0.0166(8)	0.7500	0.5276(4)
C(28)	-0.0144(6)	0.6752(4)	0.5701(3)
C(29)	-0.0697(6)	0.7965(4)	0.6360(3)
Cl(2)	0.4926(5)	0.2500	0.7260(2)
Cl(3)	0.3916(4)	0.2500	0.5800(2)
Csol	0.358(2)	0.2500	0.6726(9)
H(3)	0.2208(8)	0.5585(5)	0.4964(4)
H(4)	0.373(1)	0.4606(7)	0.5587(4)
H(5)	0.550(1)	0.510(1)	0.6334(5)
H(6)	0.5897(9)	0.664(1)	0.6495(5)
H(16)	0.3000(6)	0.8294(4)	0.3768(3)
H(17)	0.2688(8)	0.9458(5)	0.2930(4)
H(18)	0.0502(9)	1.0128(5)	0.2787(4)
H(19)	-0.1397(8)	0.9651(5)	0.3488(4)
H(20)	-0.1101(7)	0.8495(4)	0.4342(3)
H(28)	-0.0131(6)	0.6095(4)	0.5704(3)
H(29)	-0.1014(6)	0.8320(4)	0.6777(3)

TABLE 3. Crystal data and summary of data collection for [(C<sub>13</sub>H<sub>8</sub>- $\mu$ -CPh<sub>2</sub>-C<sub>5</sub>H<sub>4</sub>)ZrCl<sub>2</sub>] $\cdot$ CH<sub>2</sub>Cl<sub>2</sub>

Mol wt.	641.5
Space group	<i>Pnma</i>
Cell constants	
<i>a</i> , Å	9.671(2)
<i>b</i> , Å	15.218(4)
<i>c</i> , Å	18.695(5)
<i>V</i> , Å <sup>3</sup>	2751
Molecules/unit cell	4
<i>D<sub>c</sub></i> , g cm <sup>-3</sup>	1.55
$\mu_c$ , cm <sup>-1</sup>	2.1
Radiation	Mo K $\alpha$
Max cryst dimens, mm	0.20 $\times$ 0.25 $\times$ 0.40
Scan width, deg	0.80 + 0.20 tan $\theta$
Std reflns	600,060,008
Decay of stds	< 2%
2 $\theta$ range, deg	2–50
No reflns colld	2784
No. of obsd reflns	1752
No. of params varied	176
<i>R</i>	0.051
<i>R<sub>w</sub></i>	0.058

TABLE 5. Crystal data and summary of data collection for [(C<sub>13</sub>H<sub>8</sub>- $\mu$ -CPh<sub>2</sub>-C<sub>5</sub>H<sub>4</sub>)HfCl<sub>2</sub>] $\cdot$ CH<sub>2</sub>Cl<sub>2</sub>

Mol wt.	728.8
Space group	<i>Pnma</i>
Cell constants	
<i>a</i> , Å	9.659(2)
<i>b</i> , Å	15.211(4)
<i>c</i> , Å	18.677(4)
<i>V</i> , Å <sup>3</sup>	2744
Molecules/unit cell	4
<i>D<sub>c</sub></i> , g cm <sup>-3</sup>	1.77
$\mu_c$ , cm <sup>-1</sup>	2.1
Radiation	Mo K $\alpha$
Max cryst dimens, mm	0.10 $\times$ 0.15 $\times$ 0.20
Scan width, deg	0.80 + 0.20 tan $\theta$
Std reflns	600,060,008
Decay of stds	< 2%
2 $\theta$ range, deg	2–50
No. reflns colld	2756
No. of obsd reflns	1734
No. of params varied	176
<i>R</i>	0.038
<i>R<sub>w</sub></i>	0.043

was extracted with methylene chloride to remove LiCl. Cooling of the extract to  $-20^\circ\text{C}$  gave 13 g analytically pure crystals in 92.8% yield.

### 3.4. Preparation of 4

A similar procedure to that used for 3, but starting from HfCl<sub>4</sub> (and giving yellow product suspension) yielded analytically pure yellow crystals in 93.8% yield.

### 3.5. X-ray data collection, structure determination and refinement for [(C<sub>13</sub>H<sub>8</sub>- $\mu$ -CPh<sub>2</sub>-C<sub>5</sub>H<sub>4</sub>)ZrCl<sub>2</sub>] · CH<sub>2</sub>Cl<sub>2</sub>

Single crystals of the compound were sealed under N<sub>2</sub> in thin-walled glass capillaries as a precaution, although the crystals appear rather stable in air. Data were collected on an Enraf-Nonius CAD4 diffractometer by the  $\theta/2\theta$  scan technique as previously described [13]. A summary of data collection parameters is given in Table 3. A series of psi scans indicated no absorption correction was needed. Calculations were carried out with the SHELX system of computer programs [8]. The position of the zirconium atom was found using

standard heavy atom techniques, and subsequent difference map revealed the position of all non-hydrogen atoms. The non-hydrogen atoms were refined with anisotropic thermal parameters. Hydrogen atoms were placed in calculated positions. The CH<sub>2</sub>Cl<sub>2</sub> molecule in the lattice exhibited high thermal parameters, but it was well resolved. Refinement converged with  $R = 0.051$  and  $R_w = 0.058$ . A final difference Fourier map showed no unaccounted electron density. The positional parameters are given in Table 4, and the temperature factors and hydrogen atom coordinates are available from the Cambridge Crystallographic Data Centre.

### 3.6. X-ray data collection structure determination and refinement for [(C<sub>13</sub>H<sub>8</sub>- $\mu$ -CPh<sub>2</sub>-C<sub>5</sub>H<sub>4</sub>)HfCl<sub>2</sub>] · CH<sub>2</sub>Cl<sub>2</sub>

Data collection and structure solution and refinement were accomplished as for the zirconium analogue, with which this compound is isostructural. An empirical absorption was made. Refinement converged with  $R = 0.038$  and  $R_w = 0.043$ . A summary of data collection parameters and the positional parameters are given in Tables 5 and 6.

TABLE 6. Final fractional coordinates

Atom	x	y	z
Hf	0.17970(6)	0.7500	0.62706(2)
Cl	0.2142(3)	0.6330(2)	0.7117(1)
C(1)	0.255(1)	0.7500	0.5042(6)
C(2)	0.323(1)	0.6734(7)	0.5338(4)
C(3)	0.298(1)	0.5811(7)	0.5271(5)
C(4)	0.384(1)	0.525(1)	0.5626(6)
C(5)	0.491(2)	0.554(1)	0.6073(7)
C(6)	0.515(1)	0.640(1)	0.6169(6)
C(7)	0.431(1)	0.7018(8)	0.5815(5)
C(14)	0.116(1)	0.7500	0.4637(6)
C(15)	0.0978(9)	0.8301(5)	0.4137(4)
C(16)	0.2087(9)	0.8586(6)	0.3727(5)
C(17)	0.190(1)	0.9260(7)	0.3219(5)
C(18)	0.062(1)	0.9646(7)	0.3143(5)
C(19)	-0.048(1)	0.9368(7)	0.3551(5)
C(20)	-0.030(1)	0.8688(6)	0.4045(5)
C(27)	0.016(1)	0.7500	0.5276(6)
C(28)	-0.0134(9)	0.6743(6)	0.5698(4)
C(29)	-0.0686(9)	0.7962(6)	0.6362(4)
Cl(2)	0.4930(8)	0.2500	0.7253(3)
Cl(3)	0.3918(6)	0.2500	0.5794(3)
Csol	0.360(3)	0.2500	0.675(1)
H(3)	0.221(1)	0.5584(7)	0.4967(5)
H(4)	0.371(1)	0.460(1)	0.5572(6)
H(5)	0.550(2)	0.510(1)	0.6327(7)
H(6)	0.590(1)	0.661(1)	0.6492(6)
H(16)	0.3009(9)	0.8295(6)	0.3774(5)
H(17)	0.270(1)	0.9461(7)	0.2924(5)
H(18)	0.051(1)	1.0129(7)	0.2787(5)
H(19)	-0.140(1)	0.9650(7)	0.3486(5)
H(20)	-0.110(1)	0.8490(6)	0.4340(5)
H(28)	-0.0121(9)	0.6087(6)	0.5701(4)
H(29)	-0.1003(9)	0.8316(6)	0.6779(4)

## References

- 1 W. Kaminsky, K. Kulper, H.H. Brintzinger and F.R.P. Wild, *Angew. Chem., Int. Ed. Engl.*, (24) (1985) 507.
- 2 W. Kaminsky and H. Sinn, *Olefin polymerization*, Springer Verlag, Berlin, 1988; T. Keii and K. Soga, *Catalytic olefin polymerization*, Elsevier, Amsterdam, 1990.
- 3 J.A. Ewen, Ligand effects on metallocene catalyzed polymerizations, in T. Keii and K. Soga (eds.), *Catalytic polymerizations of olefins*, Elsevier, New York, 1986; S. Miya, T. Yoshimura, T. Mise and H. Yamazaki, *Polym. Prepr. Jpn.*, 37 (1988) 285; T. Mise, S. Miya and H. Yamazaki, *Chem. Lett.*, (1989) 1853; P. Pino, G. Consiglio, A. Sironi and M. Moret, *Organometallics*, 9 (1990) 3098; A. Razavi, Electronic and steric influence of the cyclopentadienyl substituents and the role of the bridge on the catalytic behavior of ansa metallocene complexes in stereospecific polymerizations of  $\alpha$ -olefin in homogeneous catalysis, in *Proceedings of second international business forum on specialty polyolefins*, September 22–24, 1992, 167; W. Spaleck, M. Antberg, J. Rohrmann, A. Winter, B. Bachmann, J. Behm and W.A. Herrmann, *Angew. Chem., Int. Ed. Engl.*, 10 (1992) 31.
- 4 F.S. Dyachkovskii, *Vysokomol. Soyed.*, 7 (1976) 114; R.F. Jordan, C.S. and Bajgur, R. Willet and B. Scott, *J. Am. Chem. Soc.*, 108 (1986) 7410; R. Taube and L. Krukowka, *J. Organomet. Chem. C9*, (1987) 6347; G.G. Hlatky, H.W. Turner and R.R. Eckman, *J. Am. Chem. Soc.*, 111 (1989) 2728; M. Bochmann, L.M. Wilson, M.B. Hursthouse and M. Motevalli, *Organometallics*, 7 (1988) 1148; M. Bochman, *Nacr. Chem. Tech. Lab.*, 38 (1990) 1238; X. Yang, C.L. Stern and T.J. Marks, *Organometallics*, 10 (1991) 840.
- 5 J.A. Ewen, L.R. Jones and A. Razavi, *J. Am. Chem. Soc.*, 110 (1988) 6255.
- 6 A. Razavi and J. Ferrara, *J. Organomet. Chem.*, 435 (1992) 310.
- 7 A. Razavi and U. Thewald, *J. Organomet. Chem.*, 445 (1993) 111.
- 8 J.W. Lauher and R. Hoffmann, *J. Am. Chem. Soc.*, 98 (1976) 1729.

- 9 K. Prout, T. Cameron, R.F. Forder, S.R. Critchly, B. Denton and G.V. Rees, *Acta Crystallogr., Sect. B*, **30** (1974) 2290.
- 10 P.B. Hitchcock, M.F. Lappert and C.R.C. Milne, *J. Chem. Soc., Dalton Trans.*, (1981) 180.
- 11 K.J. Ivin, J.J. Rooney, C.D. Stewart, M.L.H. Green and R. Mahtab, *J. Chem. Soc., Chem. Commun.*, (1978) 604.
- 12 M. Brookhart, M.L.H. Green and S.L.L. Wong, *Prog. Inorg. Chem.*, **36** (1988) 1.
- 13 P.L. Watson, *J. Am. Chem. Soc.*, **104** (1982) 337.
- 14 L. Clawson, J. Soto, S.L. Buchwald, M.L. Steigerwald and R.H. Grubbs, *J. Am. Chem. Soc.*, **107** (1985) 3377.
- 15 W.E. Piers and J.E. Bercaw, *J. Am. Chem. Soc.*, **112** (1990) 9406.
- 16 W. Roll, H.H. Brintzinger, B. Rieger and R. Zolk, *Angew. Chem., Int. Ed. Engl.*, **29** (1990) 279.
- 17 J. Holton, M.F. Lappert, D.G.H. Ballard, R. Pearce, J.L. Atwood and W.E. Hunter, *J. Chem. Soc., Dalton Trans.*, (1979) 46.
- 18 G.M. Sheldrick, SHELX, a system of computer programs for X-ray structure determination, 1976.